

Article

Experimental Investigation into the Combustion Characteristics of Propane Hydrates in Porous Media

Xiang-Ru Chen ^{1,2,3}, Xiao-Sen Li ^{1,2}, Zhao-Yang Chen ^{1,2,*}, Yu Zhang ^{1,2}, Ke-Feng Yan ^{1,2} and Qiu-Nan Lv ^{1,2}

¹ Key Laboratory of Gas Hydrate, Guangzhou Institute of Energy Conversion, Chinese Academy of Sciences, Guangzhou 510640, China; E-Mails: chenxr@ms.giec.ac.cn (X.-R.C.); lixs@ms.giec.ac.cn (X.-S.L.); chenzy@ms.giec.ac.cn (Z.-Y.C.); zhangyu1@ms.giec.ac.cn (Y.Z.); yankf@ms.giec.ac.cn (K.-F.Y.); lvqn@ms.giec.ac.cn (Q.-N.L.)

² Guangzhou Center for Gas Hydrate Research, Chinese Academy of Sciences, Guangzhou 510640, China

³ University of Chinese Academy of Sciences, Beijing 100083, China

* Author to whom correspondence should be addressed; E-Mail: chenzy@ms.giec.ac.cn; Tel.: +86-20-8705-8468; Fax: +86-20-8703-4664.

Academic Editor: Richard Coffin

Received: 11 November 2014 / Accepted: 26 January 2015 / Published: 5 February 2015

Abstract: The combustion characteristics of both pure propane hydrates and the mixtures of hydrates and quartz sands were investigated by combustion experiments. The flame propagation, flame appearance, burning time and temperature in different hydrate layers were studied. For pure propane hydrate combustion, the initial flame falls in the “premixed” category. The flame propagates very rapidly, mainly as a result of burnt gas expansion. The flame finally self-extinguishes with some proportion of hydrates remaining unburned. For the hydrate-sand mixture combustion, the flame takes the form of many tiny discontinuous flames appearing and disappearing at different locations. The burn lasts for a much shorter amount of time than pure hydrate combustion. High porosity and high hydrate saturation is beneficial to the combustion. The hydrate combustion is the combustion of propane gas resulting from the dissociation of the hydrates. In both combustion test scenarios, the hydrate-dissociated water plays a key role in the fire extinction, because it is the main resistance that restrains the heat transfer from the flame to the hydrates and that prevents the hydrate-dissociated gas from releasing into the combustion zone.

Keywords: propane hydrates; combustion; porous media; flame propagation

1. Introduction

Natural gas hydrates (NGH) are non-stoichiometric crystalline compounds formed by water and small gas molecules under conditions of high pressure and low temperature. NGH deposits have been discovered widely in the world, mainly in marine sediments and permafrost areas. Currently, NGH are regarded as a promising unconventional energy resource, because huge quantities of natural gas are believed to be entrapped in them [1]. Gas recovery from NGH involves the dissociation of NGH, which can be realized through shifting the *in situ* thermodynamic equilibrium conditions. Thermal stimulation, depressurization and thermodynamic inhibitor injection are the three main proposed production methods [2]. No matter what method is adopted for gas recovery, a certain amount of energy input would be necessary. Otherwise, a significant temperature decline would be inevitable [3], because the hydrate dissociation process is endothermic. Most likely, the temperature decline will lead to ice formation, slowing or even terminating further hydrate dissociation.

Steam or hot brine injection are the usual approaches of energy input. However, these methods suffer significant energy losses during the heat delivery process. By contrast, *in situ* combustion (ISC) is an innovative thermal stimulation concept proposed by Cranganu [3,4], which provides the desired heat for hydrate dissociation via a combustion reaction right within the down-hole NGH reservoirs. Schick *et al.* [5,6] developed a 425-L reservoir simulator and experimentally studied ISC for gas production from methane hydrates, which showed that about 15% of the produced methane should be consumed for all hydrates in the simulator to dissociate. Numerical simulation results indicated that this method can achieve substantial cuts in the needed energy input, with an energy efficiency of 90% [7].

The ISC methods proposed by Cranganu [3,4] and Schick *et al.* [5,6] were originally aimed at gas production from submarine hydrate reservoirs. They both adopted a closed combustion system, and there was no direct contact between the reservoir and the combustion reaction. The combustion heat is transferred to the reservoir through the wall of the combustor or heat-exchanger. By contrast, ISC would be easier for NGH reservoirs in permafrost regions, where there is much less water with which to deal. Therefore, an open process of combustion in a permafrost NGH reservoir may be possible, which can spare the use of a series of complicated combustion apparatuses. Actually, the open ISC is a well-known method for heavy oil exploitation [8,9] and underground coal gasification [10].

For the permafrost NGH dissociation and recovery using the open ISC method, the flame erupting from the burner nozzle will directly contact the NGH under the down-hole. Therefore, the great concern for this method is the safety issue. It is unclear for us whether the open ISC in the permafrost NGH reservoir will lead to the combustion of whole NGH in sediments and result in the risk of runaway fires. Although we can use the inverse diffusion flame combustion technology to avoid the leakage of oxygen or air into the production well, it is still necessary to investigate the combustion characteristics of hydrates before we can develop successful open ISC technologies for permafrost NGH exploitation. Note that it is challenging to investigate the hydrate combustion characteristics thoroughly, because the hydrate combustion process involves multi-component reactions and multi-phase changes. Moreover,

hydrates are hard to keep in normal conditions, due to their special equilibrium properties. Presently, there are only a few publications providing some fundamental knowledge on hydrate combustion. Ueda *et al.* made a series of methane hydrate combustion studies, which resembled the classic “Emmons problem” [11]. Specifically, they investigated the combustion phenomena over methane hydrates in a laminar boundary layer, both numerically and experimentally. Using a one-dimensional thermal model, they first numerically estimated the flame propagation speed over methane hydrates in a laminar boundary layer to be about 1–1.5 mm/s [12]. Then, their experimental studies showed that the flame propagation speed was in the range of 2–3 mm/s, independent of the free stream velocity [13]. Later on, they illuminated the mechanism of flame spreading over methane hydrates through combustion experiments with different hydrate surface temperatures [14,15]. Two different types of flame propagation phenomena were observed: the so-called “low speed flame spreading” at low surface temperatures, where the methane ejection velocity was slow, and “high speed flame spreading” at high surface temperatures, where the methane ejection velocity was high. In addition, Nakoryakov *et al.* [16] also conducted experiments on methane hydrate combustion, which suggested that the hydrate dissociation rates with combustion exceeded those without combustion by many times.

To investigate the combustion characteristics of natural gas hydrates, methane hydrates should be the first choice, as the majority of naturally occurring NGH are methane hydrates. However, the equilibrium temperature of methane hydrates is about $-80\text{ }^{\circ}\text{C}$ under atmospheric pressure, which means that they will decompose intensively at temperatures above $0\text{ }^{\circ}\text{C}$. To avoid vast dissociation before ignition, the methane hydrates should be kept in a liquid nitrogen condition, where the temperature can be as low as $-196\text{ }^{\circ}\text{C}$. However, such a low temperature would cause the so-called “self-preservation” effect [17], namely, in combustion experiments, an ice layer would form over the surface of the hydrates, keeping methane from leaving the hydrate structure. To avoid excessive use of liquid nitrogen, as well as the vast dissociation of hydrates before ignition, in this work, we adopted propane hydrates, which have relatively high stability, instead of methane hydrates. Although NGH may exist in various kinds of reservoirs, such as sand, shale and clay, those hydrates in sandy reservoirs are considered the most feasible for economic exploitation [18]. Presently, much model hydrate reservoir research has been done with quartz sand [19–21], and here, we also adopted quartz sand and hydrate mixtures to mimic the permafrost hydrate reservoir.

The main objective was to investigate the combustion characteristics of (1) pure propane hydrates and (2) propane hydrates mixed with different amounts of quartz sands, which are supposed to simulate the porous media in real hydrate reservoirs of different porosities and hydrate saturations. As a matter of fact, the temperatures in permafrost hydrate reservoirs are reported to be above $0\text{ }^{\circ}\text{C}$ ($8\text{--}12\text{ }^{\circ}\text{C}$ in the world-renowned Messoyakha Field [22] and $0.79\text{--}1.15\text{ }^{\circ}\text{C}$ in Qilian Mountain permafrost [23]), and for safety considerations, in this work, we conducted the combustion tests at room temperature and atmospheric pressure without the cooling of liquid nitrogen.

2. Experimental Section

2.1. Materials

The analytical pure propane gas with a purity of 99.9% was supplied by Huate Gas Co., Ltd., Foshan, China. The quartz sands were provided by Bandao Quartz Sand Factory, Guangzhou, China. The diameter of the quartz sands is about 0.30–0.45 mm. All aqueous solutions were prepared using de-ionized water, which was prepared by an ultrapure water system (Nanjing Ultrapure Water Technology Co., Ltd., Nanjing, China) with a resistivity of 18.25 M Ω ·cm.

2.2. Apparatus and Procedures

The propane hydrate samples were prepared on a self-developed experimental apparatus that has been reported in detail in our previous work [24]. In brief, the propane hydrate preparing apparatus for the hydrate formation involves a 336-mL cylindrical crystallizer with magnetic stirring, a temperature control system, a gas supply system, a data acquisition system and some temperature and pressure measurement and control units. To synthesize propane hydrate samples, the pressure inside the crystallizer and the supply vessel was set to about 3.8 bar, and the crystallizer was maintained in a 273.65 ± 0.2 K water bath for about three days. The prepared hydrate sample is the slurry of solid hydrates and liquid water, which was cooled by liquid nitrogen before being taken out of the reactor and being dealt with for the combustion experiment. All of the liquid water in the sample was frozen into ice under the lower temperature environment. The frozen solid sample was crushed to a particle size smaller than 5 mm before mixing with quartz sand. The hydrate mass fraction of the sample can be calculated by a gas state equation according to the pressure and temperature data in the reactor and the supply vessel [24]. The hydrate samples with about a 25% of hydrate mass fraction were prepared for the combustion experiment in this work.

Figure 1 is the photograph of the apparatus used for the hydrate combustion experiment in this work. Specifically, it is composed of a visual combustion chamber (a), a hydrate combustion vessel (b) with an electronic igniter and 5 thermocouples, a switch unit for the electronic igniter (c) and an Agilent Model 34970A data acquisition system (d), which is controlled by a computer (e) through the Agilent data acquisition software application, BenchLink. The combustion chamber (a) is made of a cylindrical refractory glass pipeline with two open sides. The initial temperature in the combustion chamber can be controlled by a temperature controlling water vessel built into the lower part of the combustion chamber. The combustion vessel (b) is installed in the center of the combustion chamber. Figure 2 displays the schematic of the hydrate combustion vessel (b). The vessel (150 mm in length, 30 mm in width and 50 mm in depth) is made of stainless steel with a 2-mm thickness. There are 5 orifices distributed vertically on one side of the vessel at an interval of 10 mm. Five type-K thermocouples with ± 0.1 K accuracy are inserted into the vessel to measure the temperature variation at different depths in the vessel. The five thermocouples, A, B, C, D and E, measure, respectively, the temperatures at the corresponding depths of -5 mm, -15 mm, -25 mm, -35 mm and -45 mm. An electronic igniter is located at the left end of the vessel for ignition. During the combustion test, a digital camera is set to record the combustion phenomena.

For pure propane hydrate combustion experiments, about 140-g propane hydrate samples were filled into the combustion vessel to the height of the B orifice. The surface was made level. After the vessel was set, the electronic igniter was turned on. After the hydrates were on fire, the electronic lighter was turned off. The temperature variations in the vessel were measured with the 5 type-K thermocouples and were recorded consecutively by the Agilent data acquisition system on the computer at intervals of 1 s. In the meantime, the combustion phenomena were photographed by a digital camera.

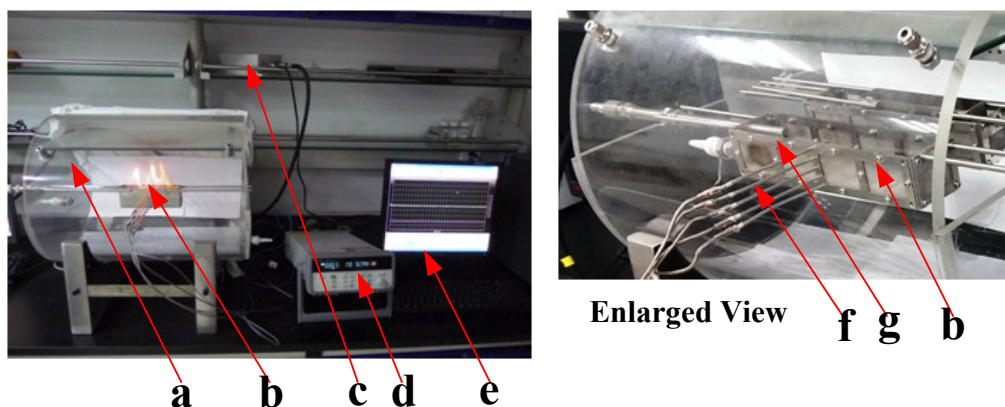


Figure 1. Hydrate combustion test apparatus. a, combustion chamber; b, hydrate combustion vessel; c, switch unit; d, Agilent 34970A data acquisition system; e, computer; f, thermocouples; g, electronic igniter.

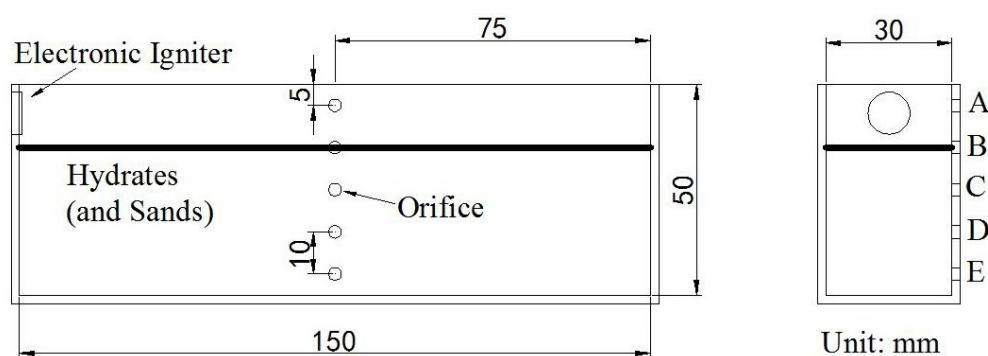


Figure 2. Hydrate combustion vessel.

For the combustion experiments of hydrate-sand mixtures, predetermined amounts of propane hydrate samples and quartz sands were mixed carefully in a liquid nitrogen environment before the combustion experiment. The sands were frozen to about $-1\text{ }^{\circ}\text{C}$ before they were mixed with the hydrate particles. Then, the mixture was packed into the combustion vessel to the height of the B orifice, which was supposed to simulate the porous media in real hydrate deposits of different porosities (Φ) and hydrate saturations (S_H). The density of the sands is $\rho_s = 2.65\text{ g/cm}^3$. The density of the hydrates is estimated as $\rho_H = 0.9\text{ g/cm}^3$.

The overall volume of the mixture is $V = 15 \times 3 \times 3.5 = 157.5\text{ cm}^3$.

The pore volume V_p is calculated as:

$$V_p = V - m_s/\rho_s \quad (1)$$

The hydrate saturation S_H is calculated as:

$$S_H = 0.25m_H/(\rho_H V_p) \quad (2)$$

Table 1 lists the mass of the hydrate samples and sands used for different porosities and hydrate saturations. The surface of the mixture was made level. The other procedures were the same as the pure hydrate combustion experiment described above. These experiments involve taking out the hydrates from the pressurized reactor, mixing propane hydrates with quartz sands under a liquid nitrogen environment and ambient pressure, filling the samples into the combustion vessel, *etc.* Many factors will result in the hydrate dissolution and sample homogeneity and affect the reproducibility of the experiments, so each case of the combustion experiment was repeated at least three times in this work.

Table 1. The mass of sand and hydrate samples for different porosities (ϕ) and hydrate saturations (S_H).

Porosity ϕ (%)	Hydrate Saturation S_H (%)	Mass of Sands m_s (g)	Mass of Hydrate Samples m_H (g)
58	15	175.5	48.6
58	11	175.5	36.5
58	7	175.5	24.3
50	15	210.6	42.1
50	11	210.6	30.8
50	7	210.6	19.5
41	15	245.7	34.8
41	11	245.7	25.5
41	7	245.7	16.2

3. Results and Discussion

3.1. Combustion of Pure Propane Hydrates

3.1.1. Combustion Characteristics

Figure 3 demonstrates the flame appearance at different times in a typical hydrate combustion test. The electronic igniter was activated at $t = 0$ s. After about 2–3 s, the flame would appear, when the propane released from the hydrate dissociation reaches the requisite concentration for combustion at the surface. The flame would then cover the entire surface of the hydrates almost instantaneously, because a continuous fuel-air layer formed over the entire surface before ignition, due to the hydrate dissociation. This suggests that the initial flame falls in the “premixed” category. The initial flame propagates very quickly, mainly as the result of burnt gas expansion. Actually, this is very much like so-called “high speed flame spreading” [17].

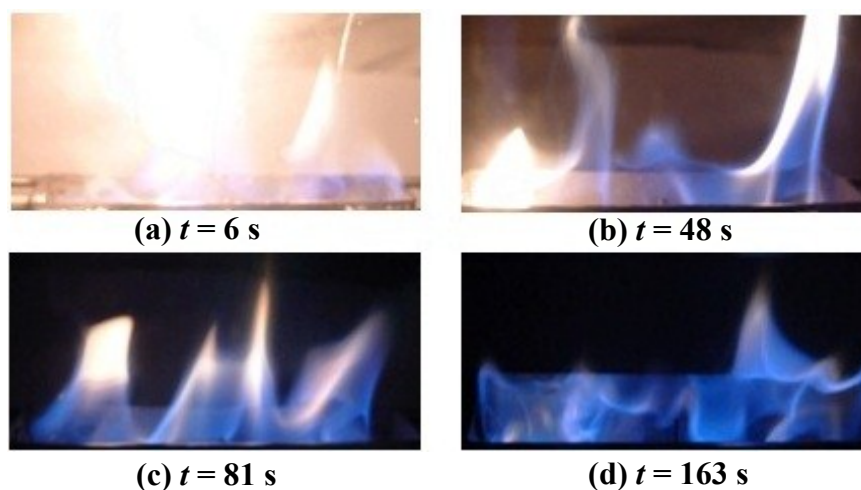


Figure 3. Flame over pure propane hydrates.

In the first few seconds after ignition, the size of the flame is quite large, and the flame oscillates with a large amplitude, even some flame blasts can be spotted, as shown in Figure 3a. The color of the flame is quite yellowish, and the flame brightens up the surroundings. This indicates that the hydrate dissociation is quite fast in this period of time, when the amount hydrate-dissociated water is very little and the flame has direct contact with the hydrates. Thus, the heat transfer from the flame is mostly consumed by hydrate dissociation rather than water evaporation. The vast propane ejection associated with the fast dissociation compels the flame to rise higher to acquire more air for further combustion.

The initial hydrate-dissociated propane is supposed to be depleted in a very short time. Then, the combustion flame turns into a diffusion flame. At this time, the heat transfer from the flame becomes the dominant driving force that accelerates the dissociation of the hydrates at the surface. After the flame moves away from the hydrate surface, the heat transfer to the hydrates declines, and the hydrate dissociation slows down; then, the flame would return back to the surface again. According to Figure 3b, the flame is still yellowish and bright at $t = 48$ s, while the size and oscillating amplitude decrease. This is because, as more hydrates dissociate with time, more hydrate-dissociated water is generated and covers the surface of the hydrates, which retards the heat flux to the lower hydrates and gas ejection. More water also means that there would be more water evaporated into the combustion zone, and the flame temperature would decrease to some extent consequently. From Figures 3c and 1d, we can see that the flame keeps diminishing with time, and the flame height and brightness is significantly smaller than before.

After about 180 s of burning, the fire extinguishes spontaneously, because there is not enough propane supplied for further combustion, in spite of the fact that there are still some hydrates left in the vessel. The hydrate-dissociated water in the vessel does not look transparent, but rather, turbid, and some samples float to the surface, as shown in Figure 4. This is caused by the copious quantities of small bubbles ascending in the water. These facts indicate that the accumulation of the hydrate-dissociated water reduces the gas ejection speed significantly.



Figure 4. Appearance after pure propane hydrate combustion.

3.1.2. Temperature Variation in the Combustion Vessel

The temperature variations in the combustion vessel were recorded by the five thermocouples, as shown in Figure 5. According to line T_A , the temperature at the depth of -5 mm increases sharply after $t = 3$ s, when the flame appears. This is because Thermocouple A is directly exposed to the flame. Additionally, this also indicates that the flame reaches Thermocouple A almost instantaneously from where it is ignited, as the flame propagation is very fast. After about 15 s of drastic increase, the rate slows down, and a fluctuation can be seen from about $t = 15$ s to $t = 40$ s. This temperature fluctuation corresponds to the relatively fierce flame oscillation of the initial combustion stage, when a flame blast occurs, as shown in Figure 3a. Actually, Thermocouple A is at the bottom of the combustion zone; as the flame moves closer to the surface with time, the temperature keeps increasing and reaches the peak at about $t = 150$ s.

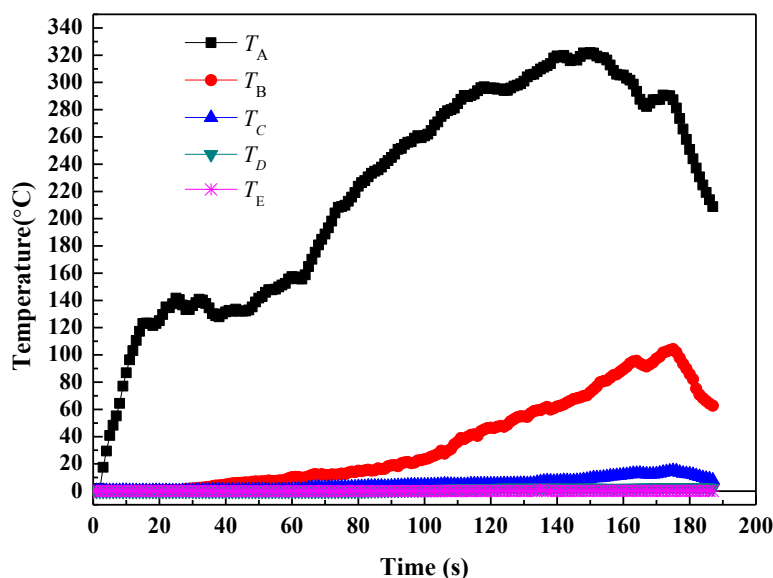


Figure 5. Temperature variation in the combustion vessel.

Thermocouple B is embedded in the hydrates right at the very surface, which is at the depth of -15 mm. We can see from line T_B that the temperature at the surface stays at 0 °C for about 20 s. During this period of time, the hydrates surrounding Thermocouple B are decomposing, and the solid ice within these hydrates is melting into liquid water. As a matter of fact, the process of vessel filling with hydrates results in the inevitable non-uniformity and roughness of the hydrates surface. Thus, the heat flux to the hydrates may not be distributed as evenly as after the surface is entirely covered by water, and the gas ejection rate is not as steady either. After the whole surface of the hydrates turns into liquid water,

the gas ejection becomes steadier than before. Then, the flame becomes relatively even, and the temperature keeps increasing, topping out at about $t = 175$ s.

From line T_C , we can see that the temperature at the depth of -25 mm also increases marginally above 0 °C as a result of heat transfer from the flame, while the temperature at the depths of -35 mm and -45 mm remains at about 0 °C almost the entire time, according to lines T_D and T_E . This coincides with the fact that there are still some portions of the hydrate samples left at the bottom of the vessel after the flame extinguishes. The flame quenches at about $t = 180$ s, and from then on, the temperatures in the vessel decline gradually.

3.2. Combustion of Propane Hydrates Mixed with Quartz Sands

3.2.1. Burning Time

Figure 6 describes the statistical data from our repeated tests regarding the average burning time of hydrate-sand mixtures for different values of porosity and hydrate saturation. According to the histogram, the burning time is generally longer for greater hydrate saturation at a constant porosity. Specifically, in the 50% porosity group, the average time of burning at $S_H = 7\%$ is 1 s, 3 s at $S_H = 11\%$ saturation and 4 s at $S_H = 15\%$. In the 58% porosity category, the average burning time at $S_H = 7\%$, 11% and 15% is 3 s, 6 s and 7 s, respectively. It is also obvious that the burning time is longer for a greater porosity at a constant saturation. This indicates that the gas ejection is generally favored by high porosity and high hydrate saturation in the hydrate-sand mixture. By contrast, the burning time is recorded as 0 s in the 41% porosity group, regardless of saturation. Only a flash of fire is spotted after the igniter is activated for a while. This means that the flame over hydrate-sand mixtures with 41% porosity cannot be sustained. Note that the burning time in this combustion test scenario is drastically shorter than pure hydrate combustion tests, as the longest time of burning is no more than 9 s, even for the highest porosity (58%) and hydrate saturation (15%). The results for different porosity cases may imply that the quartz sands with different particle sizes may have some effect on the combustion behavior, due to their different porosity, heat transfer and water seepage performances.

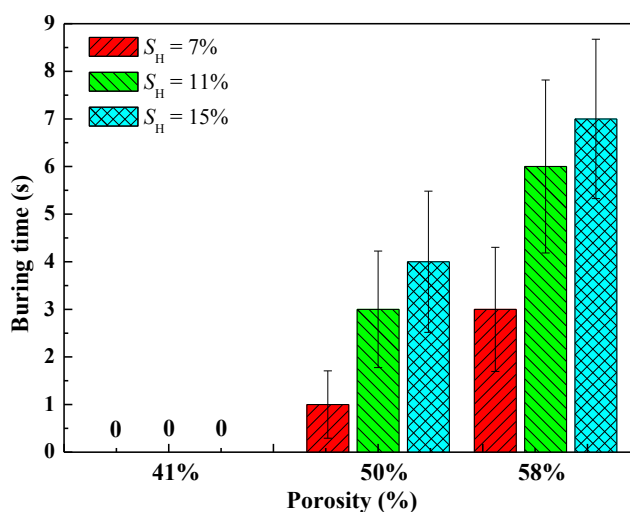


Figure 6. Burning time of propane hydrates mixed with quartz sands at different porosity and hydrate saturation levels.

3.2.2. Flame Characteristics

Figure 7 demonstrates the flame at different moments in a typical hydrate-sand combustion test with 60% porosity and 15% saturation. The flame does not appear until $t = 5$ s. Similarly, the flame propagation is very fast, mainly due to burnt gas expansion. However, the flame does not cover the entire surface of the mixture. Actually, there are many tiny discontinuous flames scattered over the surface. These tiny flames keep appearing and disappearing at different locations, and finally, all of them go out. Afterward, intensive sounds of “popping” can still be heard if one is close enough. This is because when the hydrates continue to decompose under the current experimental conditions, the hydrate-dissociated water is occupying the pores in the hydrate-sand mixture continuously, and it is becoming increasingly difficult for the propane gas to get out of the mixture. When the uppermost hydrates decompose completely, the solid ice within turns into liquid water, and the pores at the surface of the mixture are filled by a water layer. Subsequently, the gas ejection takes the form of bubbles rising and blowing through the pores at the surface. As the mixing and packing cannot guarantee absolute uniformity, both the pores and hydrate concentration are not homogeneous in the vessel. Consequently, the gas ejection at the surface is not even and steady and, so, neither are the flames. Furthermore, as the hydrates at deeper locations gradually decompose, more pores would be occupied by the hydrate-dissociated water, which would further reduce the gas permeability in the mixture.

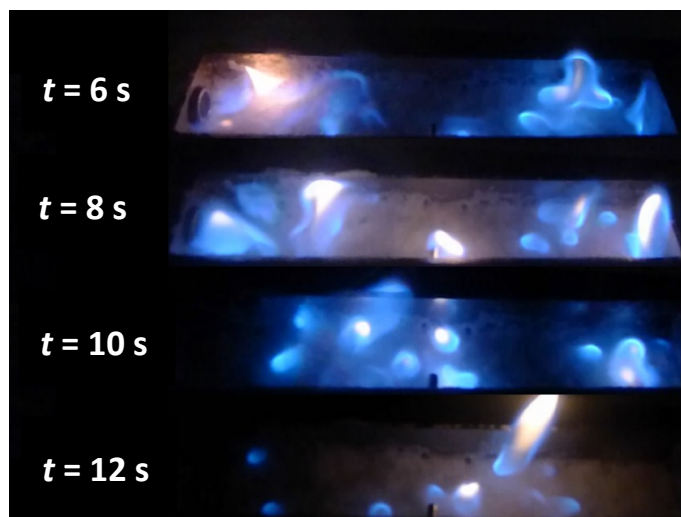


Figure 7. Flames over a hydrate-sand mixture with 60% porosity and 15% saturation.

Overall, the gas ejection is significantly restrained in this test scenario, and combustion can only be sustained for a much shorter period of time than that of pure hydrate combustion. Moreover, the very existence of sands also retards the heat flux from the flame to the hydrates. As the burn lasts for such a short period of time, the temperatures in the vessel almost remain close to 0 °C the entire time.

3.3. Mechanism of Hydrate Combustion

Figure 8 schematically depicts the combustion mechanisms of pure hydrates. The essence of hydrate combustion is the hydrate-dissociated gas combustion, since hydrates consist of gas and water molecules. The initial flame is the combustion of the gas accumulated from the hydrate dissociation

before ignition, which falls in the “premixed” category. As a result of burnt gas expansion, the initial flame propagates very fast. As the dissociation continues, the flame turns into a diffusion flame. At first, the flame has direct contact with the hydrates at the surface. The heat flux from the flame promotes hydrate dissociation. However, the water generated from hydrate dissociation impedes the heat flux to the hydrates, and the water evaporation into the combustion zone would reduce the flame temperature. The water accumulation also restrains the gas ejection process. Finally, the flame quenches, as there is not enough fuel supply. Consequently, a strengthened drainage may be beneficial to the hydrate combustion.

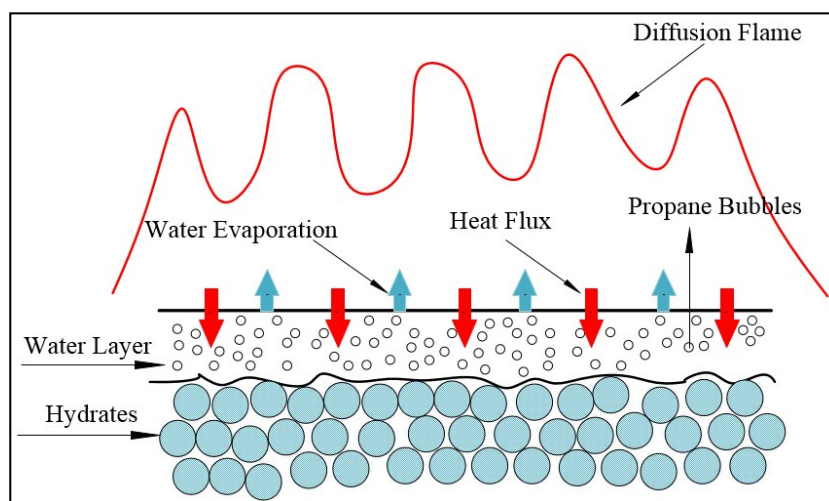


Figure 8. Schematic of pure hydrate combustion mechanisms.

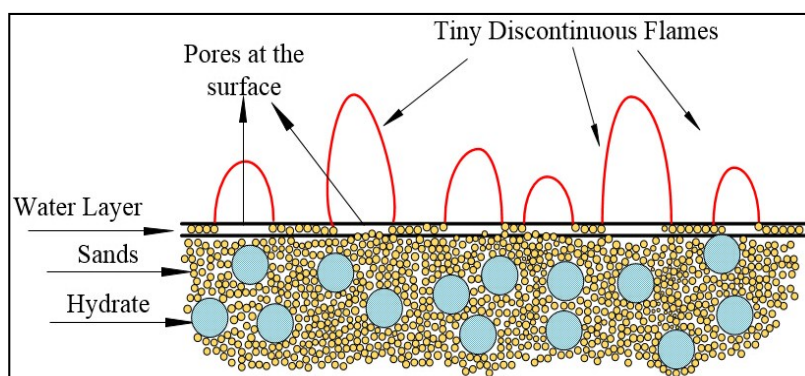


Figure 9. Schematic of hydrate-sand mixture combustion mechanisms.

Figure 9 shows the schematic of the combustion mechanisms of the hydrate-sand mixture. In this case, the gas ejection is more restrained than for pure hydrate combustion. The gas can only seep out through the pores of the mixture. After the uppermost hydrates dissociate, the pores at the surface are filled by a water layer, which would further restrain the gas ejection. The flame cannot be sustained stably and takes the form of many tiny discontinuous flames. These flames keep moving at the surface, in search for enough fuel supply. The heat transfer from the flames is both restricted by the sands and water. As a comprehensive result of these factors, the flame over the hydrate-sand mixture can only be sustained for a very short period of time, and the flame size and brightness are considerably less than for pure hydrate combustion. The hydrate-dissociated water accumulation plays a key role in the fire extinction, which indicates that the existence of the water in NGH sediments would reduce the possibility

of runaway fires. At the same time, the porosity and hydrate saturation also have an important effect on the combustion of the hydrate-sand mixture.

4. Conclusions

The combustion characteristics of pure propane hydrates and hydrate and quartz sand mixtures were experimentally investigated in this work. In pure hydrate combustion tests, the flame propagation is too fast to be distinguished at first, mainly as a result of burnt gas expansion. The flame self-extinguishes despite the fact that some portion of the hydrates are left unburned due to the accumulation of hydrate-dissociated water. In hydrate-sand mixture combustion tests, the burning time, flame size and brightness are all markedly less than those in pure hydrate combustion tests. The burn takes the form of many tiny discontinuous flames appearing and disappearing at different locations. The burn time becomes longer at the conditions of higher porosity and higher hydrate saturation. In essence, hydrate combustion is the combustion of the hydrate-dissociated gas. The combustion process is generally favored by the high rates of hydrate dissociation and the gas ejection. The hydrate-dissociated water plays a vital role in this process, since the accumulation of water significantly restrains both the heat transfer from the flame to the hydrates and the gas ejection into the combustion zone.

Acknowledgments

This work was supported by grants from the National Natural Science Foundation of China (51276182), the National Science Fund for Distinguished Young Scholars of China (51225603), the Key Arrangement Programs of the Chinese Academy of Sciences (KGZD-EW-301-2) and the China Scholarship Council (CSC201304910159), which are gratefully acknowledged.

Author Contributions

All of the authors contributed to publishing this paper. Xiang-Ru Chen, Xiao-Sen Li and Zhao-Yang Chen conceived of and designed the experiments. Xiang-Ru Chen, Zhao-Yang Chen and Yu Zhang performed the experiments and wrote the paper. Ke-Feng Yan and Qiu-Nan Lv prepared the experiments and analyzed the data.

Conflicts of Interest

The authors declare no conflict of interest.

References

1. Sloan, E.D.; Koh, C.A. *Clathrate Hydrates of Natural Gases*, 3rd ed.; CRC Press: Boca Raton, FL, USA, 2008.
2. Moridis, G.J. Numerical studies of gas production from methane hydrates. *SPE J.* **2003**, *8*, 359–370.
3. Cranganu, C. *In-situ* thermal stimulation of gas hydrates. *J. Pet. Sci. Eng.* **2009**, *65*, 76–80.
4. Cranganu, C. A method for producing natural gas from gas hydrate deposits. In Proceedings of the AAPG Annual Convention, Calgary, AB, Canada, 19–22 June 2005.

5. Schicks, J.M.; Spangenberg, E.; Giese, R.; Steinhauer, B.; Klump, J.; Luzi, M. New approaches for the production of hydrocarbons from hydrate bearing sediments. *Energies* **2011**, *4*, 151–172.
6. Schicks, J.M.; Spangenberg, E.; Giese, R.; Luzi-Helbing, M.; Priegnitz, M.; Beeskow-Strauch, B. A counter-current heat-exchange reactor for the thermal stimulation of hydrate-bearing sediments. *Energies* **2013**, *6*, 3002–3016.
7. Castaldi, M.J.; Zhou, Y.; Yegulalp, T.M. Down-hole combustion method for gas production from methane hydrates. *J. Pet. Sci. Eng.* **2007**, *56*, 176–185.
8. Reed, R.L.; Reed, D.W.; Tracht, J.H. Experimental aspects of reverse combustion in tar sands. *Trans. Soc. Pet. Engrs. AIME* **1960**, *219*, 99–108.
9. Yang, X.; Gates, I.D. Design of hybrid steam-in situ combustion bitumen recovery processes. *Nat. Resour. Res.* **2009**, *18*, 213–233.
10. Shafirovich, E.; Varma, A. Underground coal gasification: A brief review of current status. *Ind. Eng. Chem. Res.* **2009**, *48*, 7865–7875.
11. Emmons, H.W. The film combustion of liquid fuel. *ZAMM-J. Appl. Math. Mech./Z. Angew. Math. Mech.* **1956**, *36*, 60–71.
12. Kitamura, K.; Nakajo, K.; Ueda, T. Numerical calculation of a diffusion flame formed in the laminar boundary layer over methane-hydrate. In Proceedings of the 4th International Conference on Gas Hydrate (ICGH 2002), Yokohama Symposia, Yokohama, Japan, 19–23 May 2002; pp. 1055–1058.
13. Nakamura, Y.; Katsuki, R.; Yokomori, T.; Ohmura, R.; Takahashi, M.; Iwasaki, T.; Uchida, K.; Ueda, T. Combustion characteristics of methane hydrate in a laminar boundary layer. *Energy Fuels* **2009**, *23*, 1445–1449.
14. Maruyama, Y.; Yokomori, T.; Ohmura, R.; Ueda, T.; Takahashi, M.; Iwasaki, T.; Uchida, K. Flame spreading over combustible hydrate in a laminar boundary layer. In Proceedings of the 7th International Conference on Gas Hydrates (ICGH 2011), Edinburgh, Scotland, UK, 17–21 July 2011.
15. Maruyama, Y.; Fuse, M.J.; Yokomori, T.; Ohmura, R.; Watanabe, S.; Iwasaki, T.; Iwabuchi, W.; Ueda, T. Experimental investigation of flame spreading over pure methane hydrate in a laminar boundary layer. *Proc. Combust. Inst.* **2013**, *34*, 2131–2138.
16. Nakoryakov, V.E.; Misyura, S.Ya.; Elistratov, S.L.; Manakov, A.Yu.; Shubnikov, A.E. Combustion of methane hydrates. *J. Eng. Thermophy.* **2013**, *22*, 87–92.
17. Takeya, S.; Ebinuma, T.; Uchida, T.; Nagao, J.; Narita, H. Self-preservation effect and dissociation rates of CH₄ hydrate. *J. Crystal Growth* **2002**, *237–239*, 379–382.
18. Collett, T.S. Reservoir controls on the occurrence and production of gas hydrates in nature. In Proceedings of the Offshore Technology Conference, Houston, TX, USA, 4 May 2014; doi:10.4043/25242-MS.
19. Li, X.S.; Yang, B.; Li, G.; Li, B.; Zhang, Y.; Chen, Z.Y. Experimental study on gas production from methane hydrate in porous media by huff and puff method in Pilot-Scale Hydrate Simulator. *Fuel* **2012**, *94*, 486–494.
20. Fitzgerald, G.C.; Castaldi, M.J.; Zhou, Y. Large scale reactor details and results for the formation and decomposition of methane hydrates via thermal stimulation dissociation. *J. Pet. Sci. Eng.* **2012**, *94–95*, 19–27.

21. Konno, Y.; Jin, Y.; Shinjou, K.; Nagao, J. Experimental evaluation of the gas recovery factor of methane hydrate in sandy sediment. *RSC Adv.* **2014**, *4*, 51666–51675.
22. Makogon, Y.F.; Holditch, S.A.; Makogon, T.Y. Russian field illustrates gas-hydrate production. *Oil Gas J.* **2005**, *103*, 43–47.
23. Li, X.S.; Li, B.; Li, G.; Yang, B. Numerical simulation of gas production potential from permafrost hydrate deposits by huff and puff method in a single horizontal well in Qilian Mountain, Qinghai province. *Energy* **2012**, *40*, 59–75.
24. Li, X.S.; Xia, Z.M.; Chen, Z.Y.; Wu, H.J. Precombustion capture of carbon dioxide and hydrogen with a one-stage hydrate/membrane process in the presence of tetra-n-butylammonium bromide (TBAB). *Energy Fuels* **2011**, *25*, 1302–1309.

© 2015 by the authors; licensee MDPI, Basel, Switzerland. This article is an open access article distributed under the terms and conditions of the Creative Commons Attribution license (<http://creativecommons.org/licenses/by/4.0/>).